Machining-induced characteristics of microstructure-supported LPBF-IN718 curved thin walls

Sarvesh Kumar Mishra[a,b*], Gaizka Gómez-Escudero[a], Haizea González-Barrio[a], Amaia Calleja-Ochoa[a], Silvia Martinez[c], Michael Barton[b], Luis Norberto Lopez de Lacalle[b,c]

[a]*Department of Mechanical Engineering, University of the Basque Country (UPV/EHU),Plaza Torres de Quevedo, 48013, Bilbao, Spain*
[b] *Basque Center for Applied Mathematics, Mazarredo Zumarkalea, 14, 48009 Bilbo, Biscay, Spain*
[c] *Center for Advanced Aerospace Fabrication Parque Tecnológico de Bizkaia, 202, 48170, Biscay, Spain*

* Corresponding author Tel.: +34-671-32-0024; *E-mail address:* mishra.sarvesh8@gmail.com

Abstract

The microstructure-supported design of engineering components is recently gaining attention due to their high strength-to-weight and high stiffness-to-weight properties. The present study investigates the hybrid manufacturing of Inconel 718 curved thin walls with internal microstructural supports fabricated by laser powder bed fusion (LPBF). Printed walls contain a fixed curvature and thickness, whereas the internal microstructures were varied at different inclination angles. In this research, a finish milling operation has been performed at different milling parameters. Machining-induced damages on the internal microstructures have been studied and correlated with geometrical deviation and surface integrity features on the outer thin wall surfaces.

Keywords: Hybrid Manufacturing; Inconel 718; Milling

1. Introduction

Inconel 718 superalloy has been considered as a workhorse to the aerospace industry. Excellent mechanical properties at elevated temperature, high strength, and excellent thermal fatigue and oxidation resistance have proved its inevitable application in high-temperature compressor and turbine segments of aero-engines [1]. IN718 alloy qualifies to be recommended as one of the most desirable materials for use in aero-engines but with a slight compromise with density. A high density of IN718 alloy components delimits overall component weight, fuel consumption, and resulting emission levels.

Recently concluded COP26 in Glasgow [2] has confirmed an agreement amongst major countries to limit global warming to $< 2℃$ (preferably $1.5℃$). Beyond the projected global warming limit, every fractional increase in temperature will lead to the loss of lives and livelihoods. It becomes the responsibility of manufacturing researchers and aerospace industries to contribute to these goals with a sustainable strategy. The European aerospace manufacturing industry has a keen interest in developing design methodology for weight reduction of existing components, development of alternate lightweight high-performance materials, and efficient fuel usage to contribute towards these goals.

Recent advancements have focused on developing lightweight structural components with an improved design of solid parts having internal lattices (cells or microscopic internal structures) [3,4]. Load-dependent material distribution on a part has been proposed owing to the component's functional requirement and intended application [5]. Additive manufacturing plays a vital role in producing such engineered components irrespective of design complexities and restrictions on features (size, shape, orientation, etc.).

Laser powder bed fusion (L-PBF) based additive manufacturing has shown immense potential in metal printing, especially for Ti- and Ni-based superalloys [6]. Fully dense and distortion-free IN718 components have been printed by optimizing the LPBF process parameters. However, the inherent process controls have implications on the surface finish of the LPBF printed parts which necessitate the use of secondary finishing processes for final component manufacturing. The surface finish of the printed parts can be improved by electropolishing, secondary laser processing, and mechanical finishing processes [7]. Finish milling is one such process that can help in the secondary processing of complex curved surfaces. The well-established research field in the milling of superalloys will complement the additively manufactured components to help towards a more inclusive hybrid manufacturing domain.

The present study is a novel attempt in the direction of hybrid manufacturing of lightweight IN718 superalloy components. The internal microstructure supported small-scale curved component has been designed analogical to casing and static airframe components. The limiting internal microstructure feature size ($< 200\ \mu m$) for powder bed fusion of IN718 has been tested for fabrication. The developed microstructures have been employed to support the thin walls at varying orientations from the wall surface. The geometrical accuracy for printed thin-walled parts with different microstructure orientations ($0°, 60°\ and\ 120°$from the milling direction) has been compared with an LPBF printed solid thin wall. Finish milling has been performed and the geometrical accuracy has been recorded.

Nomenclature

LPBF	Laser powder bed fusion
CAD	Computer-aided drawing
IN718	Inconel 718
WC/Co	Tungsten carbide
CMM	Coordinate measuring machine

2. Materials and methods

Pre-alloyed IN718 powder with D10, D50, and D90 diameters of 17.1 μm, 32.6 μm *and* 54.8 μm respectively, has been used. The chemical composition of the powder consists of Ni (54.14%), Cr (18.40%), Fe (17.42%), Nb (4.85%), Mo (3.03%), and other elements in traces. Thin cylindrical walls are modeled and printed with internal microstructures. The part placement on the build platform and details of the part dimensions are shown in Fig. 1.

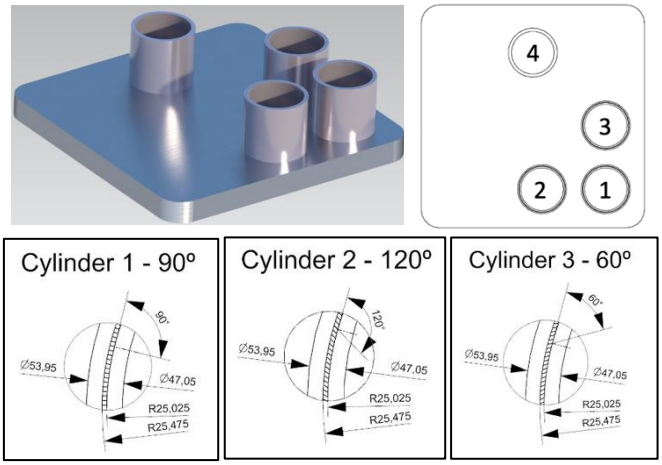

Fig. 1 CAD model and dimensions of the printed parts

AM400 (Renishaw UK) laser melting system has been used for manufacturing thin-walled pieces on a mild steel platform ($250\ mm \times 250\ mm \times 20\ mm$) using IN718 pre-alloyed powder (80% particles are 100% spherical). AM400 uses a Yttrium fiber laser with 400 W maximum power in continuous mode and the movement to the laser beam is guided by a 3D galvanometer scanning system. LPBF processing parameters for different features are provided in Table 1. Inner and outer wall thickness have been kept to 1.5 mm, whereas the internal microstructure has a length of 0.5 mm in between inner and outer thin walls. The separate strategies for LPBF of thin walls and internal microstructures have been visualized in Fig. 2. Prior to milling, the printed parts follow the solution annealing at 954 ℃ for 1 h, quenching and precipitation at 718 ℃ for 8 h, furnace cooling to 621 ℃ for 8 h 49 min, and holding 1 h 11 min in order to relieve the internal stresses.

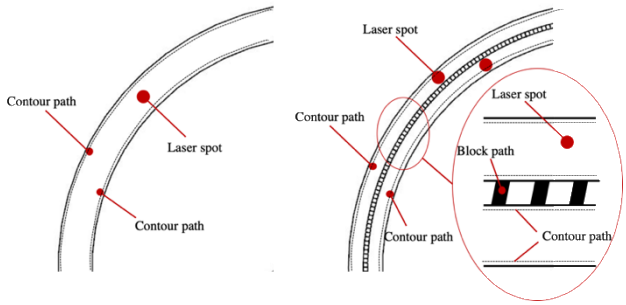

Fig. 2 Scan strategies for designed parts (with and without internal microstructures)

Table 1. LPBF process parameters and dimensions of the printed parts

Process parameters	Thin walls	Internal microstructure
Laser power (W)	200	124
Scan strategy	Stripe	Single line
Exposure time (μs)	80	40
Point distance (μm)	70	20
Hatch distance (μm)	90	-
Layer thickness (μm)	60	60
Dimensions (mm)/ orientation	Outer diameter 54	Thickness 0.2
	Inner diameter 47	Length 0.5
	Wall thickness 3.5	Orientation 0°, 60° *and* 120°

Finish milling (outer diameter) of the printed parts has been performed at Kondia A6 (3-axis, Siemens 11KW, maximum RPM 15000, Fagor 8070 controller, precision encoders with 10 μm resolution). WC/Co end mills (3 flutes, $\emptyset 8 mm$, helix angle 42°, fine grade carbide, Mikron tools - Germany) have been used for milling under flood cooling environment (emulsion oil, 1:10 oil to water ratio). Flood cooling has been selected to avoid any untoward thermal influences from the machining process. Experimental parameters for milling tests are provided in Table 2. Only the outer surface of the parts has been milled. Cutting forces were measured using a tri-axial dynamometer (Kistler 9255B, sampling frequency 16.4 kHz, Switzerland). Vickers microhardness ($HV_{0.03}$) has been measured at the subsurface of the machined surface and microstructured region to evaluate the integrity of the machined thin walls using Future-Tech HM800 hardness tester. The diamond indenter has been used at 30 g load and 12 sec dwell period.

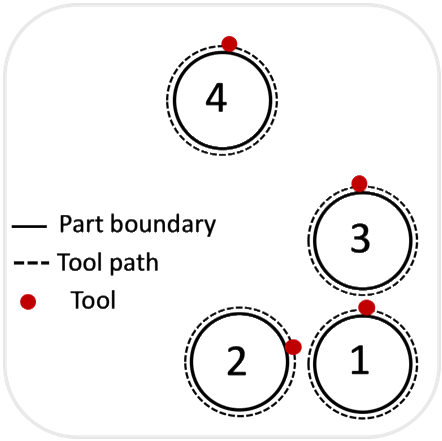

Fig. 3 Outer diameter milling of the printed parts

Post-machining measurement for the geometrical accuracy has been performed using a CMM (Zeiss MC850, Germany) with a ceramic stylus ($\emptyset 3\ mm$) having 1 μm positional accuracy. The markers have been located equidistant from the top reference surface of the build part in the z-direction. The stylus is allowed to traverse in the radial direction to collect the data at multiple locations before and after machining (Fig. 4). The average outer diameter of the measured parts has been plotted. Mitutoyo optical microscope (Mitutoyo TM505, Japan) has been used to analyze the surface after machining and polishing.

Table 2. Parameters for finish milling of the printed parts

Process parameters	Value
Milling speed (v_c, m/min)	60, 80, 100
Feed (f, mm/rev)	0.015, 0.02, 0.025
Axial depth of cut (a_p, mm)	2
Radial depth of cut (a_r, mm)	0.5

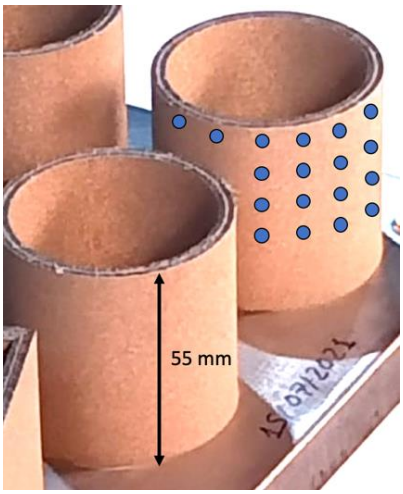

Fig. 4 CMM measurement illustration of the LPBF parts

3. Results and discussion

3.1. Optical microscopy of the internal microstructures

Fig. 5 shows the post-milling internal microstructure of printed IN718 thin walls. No damage to the internal microstructure supports has been observed for all the printed parts. Under the selected parametric conditions, tangential milling forces have not offered any internal macroscopic part damage (fracture, detachment of the microstructures, bending/deflection of the walls). In order to further test the sustenance of microstructures under the high normal milling loads, surface milling of one of the parts has been performed. In the case of the printed wall with 60° microstructure orientation, the top surface of the part (in the axial direction of the wall) has been milled to observe the influence of the normal forces on the macroscopic integrity of microstructures. There has been no perceivable damage to the microstructures, e.g., breakage, fracture, and detachment from the inner/outer walls. However, in instances, the microstructures are filled with chip fragments and burrs due to the space available between the neighboring structures.

3.2. Milling forces

The downward force (z-axis along the tool longitudinal axis) has been ignored in calculating the average milling force. With increasing milling speed, thermal softening has been supposed to dominate the deformation process and lower the milling forces [8]. However, in the present study, an increase in cutting forces with cutting speeds is perceived. One possible explanation for this behavior could be the lack of thermal softening because of the application of the flood cooling method. The dominant behavior in the absence of thermal softening is a high rate of strain hardening of IN718 alloy with increasing milling speed (deformation or strain rate). Strain hardening and material anisotropy along a particular direction have been observed in IN718 LPBF printed parts, which can be attributed to such behavior [9].

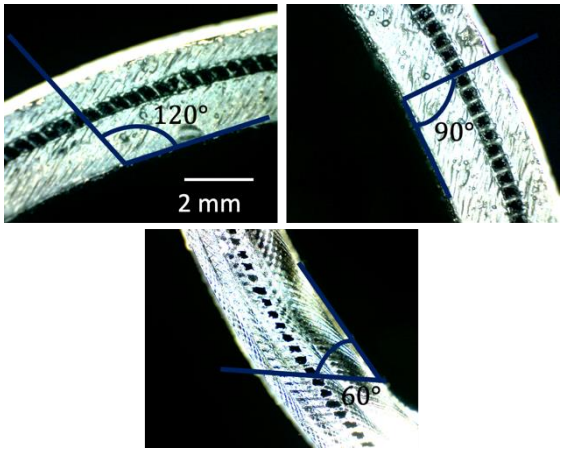

Fig. 5 Optical micrograph of the microstructure-supported thin walls

The average force plot (Fig. 6) illustrates the preliminary influence of the microstructure-supports on the milling process signature. The pieces with internal microstructures (at any orientation) have offered lower resistance to the cutting process compared to that of the solid thin wall. This observation has been recorded at constant radial and axial depth of cut values. There is no discernible flexion/distortion to the walls during the milling process.

The recorded forces throughout the process are $< 40\ N$, which further discards the possibility of appreciable elastic deformation (radial inward direction/transverse to the tool rotation axis) of the walls during the milling process. The evaluation of the dynamic components (fluctuation in maximum and minimum force values) has depicted no drastic variation throughout the milling process, which confirms the lack of perceivable elastic deflection.

The least forces are obtained for microstructures oriented either at a perpendicular or at an obtuse angle to the tool approaching direction (from the axis tangent at the inner periphery of the wall). The part with microstructure-supports oriented at 60° has a comparatively higher milling force than the other two cases. The resistance offered by the microstructure-supports at 60° orientation can be suggested as one possible explanation for higher milling forces. The behavior in the milling forces for different microstructure-supports has been explained in Fig. 7.

Higher resistance could be offered during the shearing process for microstructures at 60°, whereas the same could be lessened by administering the microstructure supports at 90°. Experimental results have proposed that 90° microstructure orientation is the best for desirable shearing (tangential milling force). The observations on milling forces are supported by a concept presented in Fig. 7 as an initial approach; however, a more detailed analysis is desired by varying the microstructure inclination from 10° to 90° at close intervals and correlating the findings on cutting forces with machining outputs. The

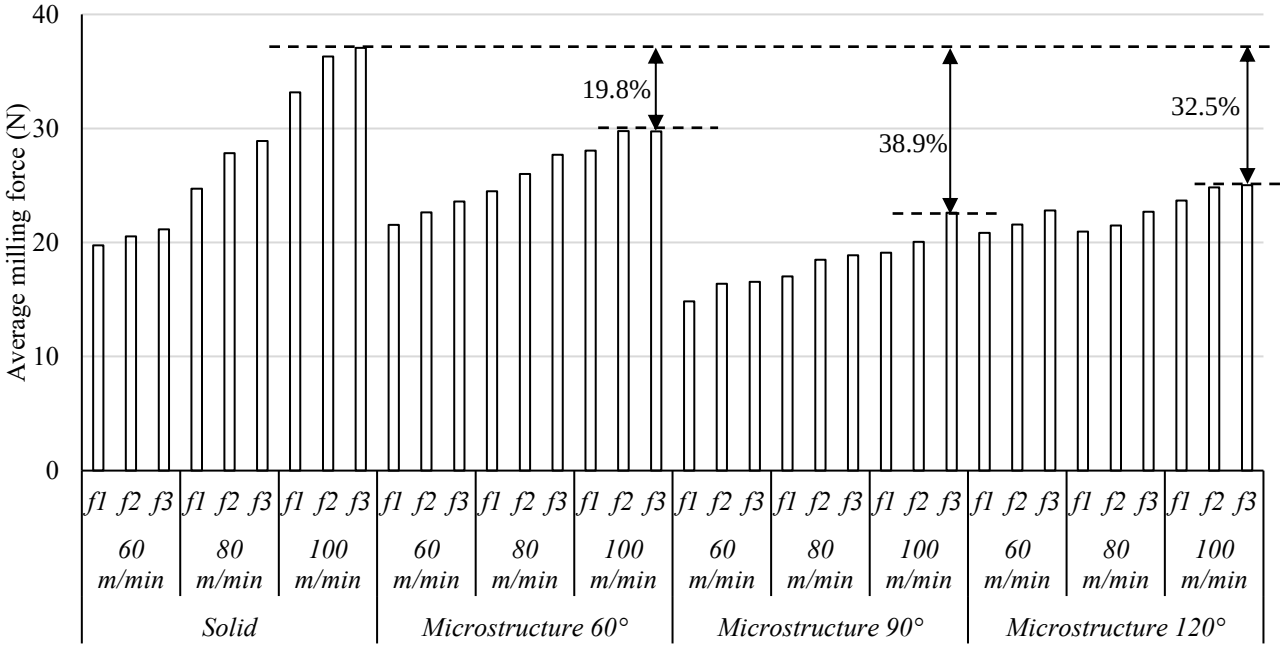

Fig. 6 Variation of forces for different pieces under varying milling conditions

geometrical accuracy has been measured in the next section to further explain the influence of microstructure inclination and support the proposed concept of reduced machining forces with microstructure orientation.

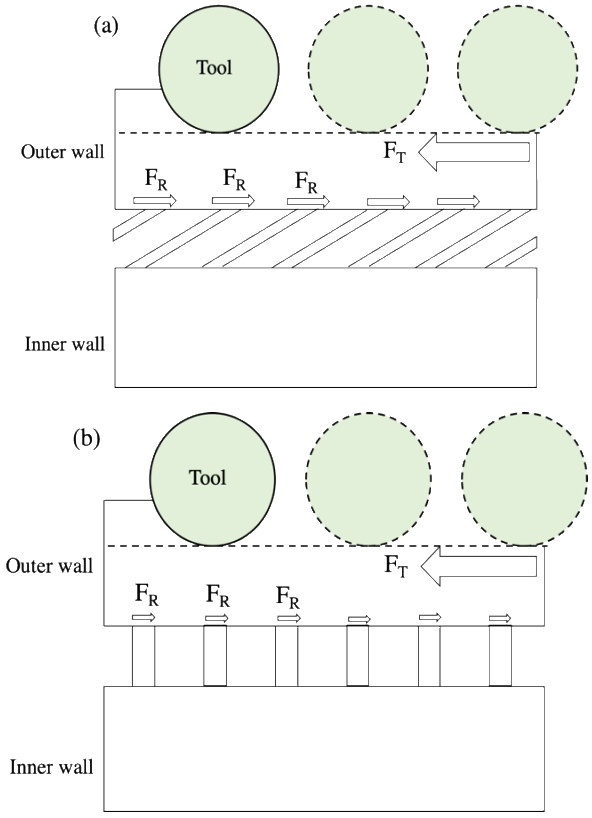

Fig. 7 Schematic of the influence of microstructure-support orientation on resistance to the milling forces for (a) 60° and (b) 90° (F_R: Resistance forces, F_T: Tangential milling force)

3.3. Geometrical accuracy of the machined components

Fig. 8 shows the deviation in the measured outer diameter of the parts. The diametral deviation under different milling conditions spans $2\ \mu m - 55\ \mu m$, which is high considering the achieved range of milling loads ($< 40\ N$). The variation in the diametral deviation is high for microstructures at 100 m/min compared to other milling speeds (shown with the help of error bars in the measurement). In the case of microstructures oriented at 60° and 90°, the variation is high (at f = 0.025 mm/rev). Maximum variations are achieved at all feed values for parts with microstructure-supports at 120°.

The reasons for such deviations in the measured diameter of the finished part can be:

a) Residual stresses in the printed parts
b) Machining induced compression to the outer wall
c) Compression and plastic deformation of the internal microstructures (administered between inner and outer walls)
d) Measurement error caused by selection of local points along the length (axis) of the cylindrical walls
e) Measurement error

The residual stress of LPBF printed superalloy components is one of the major issues affecting the accuracy of the finished components. Yet, the measurement of residual stresses and their impact on the geometrical deviation of components is out of scope in the present study. Repeatability of the measurement has been ensured by calibrating the CMM with the provided standards. Also, repeatability and reproducibility in the measurement have been ensured by recording multiple data points. Hence, the effect of points (a) and (e) can be ignored. In this study, we tested the feasibility of printing IN718 parts with internal microstructure supports ($< 200\ \mu m$), analysis of the milling forces, macroscopic damages to the printed thin walls/internal supports, and post-milling form error.

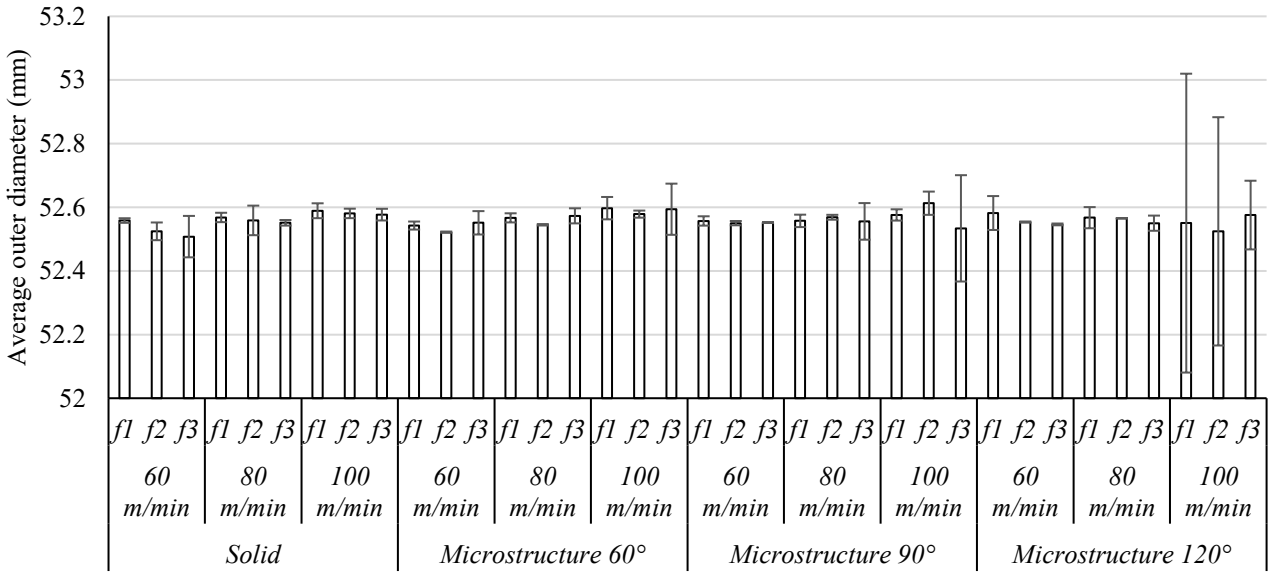

Fig. 8 Post-milling outer diameter of the parts

Machining-induced loads can be one of the major factors along with the macroscopic damages to the internal microstructure supports. In order to understand this behavior, the machined parts have been carefully sectioned and polished. Pre-and post-machined microstructure supports have been depicted in Fig. 9. No damage to the internal microstructures is seen. However, grey areas inside microstructures have appeared, which correspond to internal space filled by molten powders and entrapped metal powders from the LPBF process. Also, the top milled surface of thin-wall with 60° orientation of microstructures and corresponding machined cross-section has no damage to the microstructure supports (Fig. 10). The entrapped powders inside the microstructures have stuck to the walls (solid and microstructure supports), leaving powder-filled space between consecutive supports in some instances.

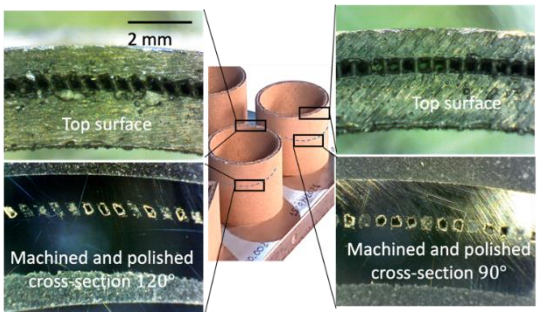

Fig. 9 Post milling analysis of the thin-walled parts top surface and sectioned milled surface (100 m/min, 0.025 mm/rev)

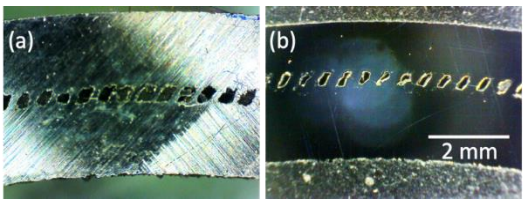

Fig. 10 (a) Surface milled top surface of the microstructured thin wall (60° orientation) and (b) final cross-section after outer diameter milling (100 m/min, 0.025 mm/rev)

To comment on the integrity against the machining-induced loads, the microhardness of the LPBF thin-walled part has been measured (Fig. 11). Sample from a part with internal microstructure at 90° orientation (machined at highest speed and feed) has been prepared to evaluate the sub-surface machining characteristics. Microhardness values at the microstructure section for as printed and machined parts are 481 ± 3.6 HV and 478 ± 1.3 HV, respectively. There is no change in the hardness of the microstructured section of the thin wall before and after machining.

The microhardness values for the machined surface become equal to the base hardness value around $600 - 650\ \mu m$ below the milled surface. Microhardness of the outer wall sections below $< 100\ \mu m$ from the top surface for as printed and machined conditions are 489 ± 4.2 HV and 512 ± 2.4 HV, respectively. The results suggest that the internal microstructure neither gets damaged under the machining loads nor the machining influences its microhardness.

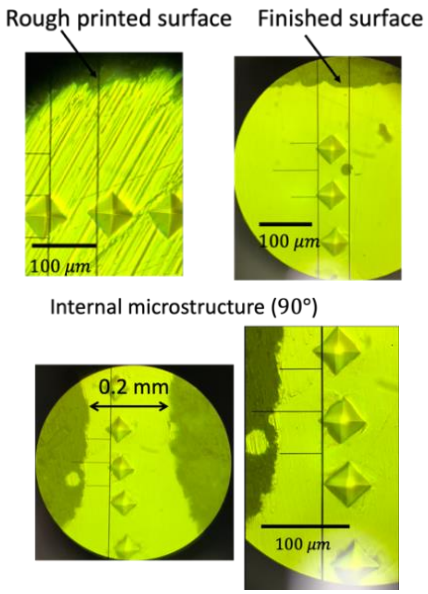

Fig. 11 Microhardness of the LPBF IN718 and machined parts

4. Conclusions and future outlook

The study presents an approach to develop lightweight IN718 printed parts using the LPBF method. The hybrid manufacturing strategy for lightweight IN718 components has been presented. The influence of microstructure-support orientations in finish milling operation has been studied. The study presents the following conclusions:

1. Finish milling doesn´t damage the macroscopic integrity of the internal microstructure supports. No breakage, detachment, or fractured supports were detected.
2. Compared to solid LPBF-IN718 thin walls, average milling forces have been reduced by 19.8 – 38.9%.
3. Microstructure orientation (90°) has offered the least average milling forces, which are in coherence with the desirable shearing forces required for finishing. A more detailed analysis of the correlation between the microstructure inclination angles and machining parameters can be further conducted to exploit the advantages offered by internal microstructure.
4. Diametral deviation in the milled parts spans $2\ \mu m - 55\ \mu m$ and maximum deviation is achieved for parts with microstructure-supports at 120°.
5. No change in the microhardness at the microstructure section is evident for printed and machined IN718 thin walls. $HV_{0.03}$ of the machined thin wall equals the printed IN718 hardness at $600 - 650\ \mu m$ below the machined surface.
6. A scope for investigating the elastic deflection of microstructure supported walls and residual stresses in the printed and milled parts has been outlined.

5. Acknowledgment

The authors acknowledge the H2020-FETOPEN-2018-2019-2020-01 ADAM^2 (Analysis, Design, And Manufacturing using Microstructures) European Union's Horizon 2020 research and innovation program (agreement No. 862025), the ELKARTEK funding program (KK-2020/00102),

References

[1] Fernández-Valdivielso A, López de Lacalle LN, Urbikain G, Rodriguez A. Detecting the key geometrical features and grades of carbide inserts for the turning of nickel-based alloys concerning surface integrity. Proc Inst Mech Eng Part C 2015;230:3725–42.

[2] COP26-Report: The Negotiations Explained. Glasgow: 2021.

[3] Liu J, Gaynor AT, Chen S, Kang Z, Suresh K, Takezawa A, et al. Current and future trends in topology optimization for additive manufacturing 2018:2457–83.

[4] Calleja-ochoa A, Gonzalez-barrio H, de Lacalle NL, Martínez S, Albizuri J, Lamikiz A. A new approach in the design of microstructured ultralight components to achieve maximum functional performance. Materials (Basel) 2021;14:1–12.

[5] Dong G, Tang Y, Zhao YF. A Survey of Modeling of Lattice Structures Fabricated by Additive Manufacturing. J Mech Des 2017;139.

[6] Cobbinah PV, Nzeukou RA, Onawale OT, Matizamhuka WR. Laser powder bed fusion of potential superalloys: A review. Metals 2021;11:1–37.

[7] Jiménez A, Bidare P, Hassanin H, Tarlochan F, Dimov S, Essa K. Powder-based laser hybrid additive manufacturing of metals: a review. Int J Adv Manuf Technol 2021;114:63–96.

[8] Liao YS, Lin HM, Wang JH. Behaviors of end milling Inconel 718 superalloy by cemented carbide tools. J Mater Process Technol 2008;201:460–5.

[9] Pérez-Ruiz JD, de Lacalle LNL, Urbikain G, Pereira O, Martínez S, Bris J. On the relationship between cutting forces and anisotropy features in the milling of LPBF Inconel 718 for near net shape parts. Int J Mach Tools Manuf 2021;170.